Grazing incidence X-rays reflectometry and diffraction studies of radiofrequency sputter deposited a-C/W interfaces

H.S. Ousmane, E. Ech-chamikh, M. Azizan, Y. Ijdiyaou and A. Essafti

Laboratoire de Physique du Solide et des Couches Minces, Faculté des Sciences Semlalia, Université Cadi ayyad, BP : 2390, Marrakech 4000, Maroc

Abstract: Amorphous carbon on tungsten (a-C/W) bi-layers have been deposited, on crystalline silicon substrates, by Radio-Frequency (RF) sputtering. Carbon films were deposited, from a high purity graphite target, with a RF power of 250 Watts; while those of tungsten were obtained, from a pure tungsten target, at two different RF powers of 100 and 200 Watts. Annealing effects, at 1000 K in vacuum, on the structure and the interface state of the samples, were studied by Grazing Incidence X-rays Reflectometry (GIXR) and Diffraction (GIXD) techniques. The GIXR measurements show that the raw a-C/W interfaces are abrupt while the annealed ones are diffuse with formation of a W2C interfacial layer. The GIXD measurements reveal that W films deposited at 100 Watts are amorphous whereas those deposited at 200 Watts are polycrystalline in the β-W phase. After annealing at 1000 K, the formation of W_2C at the a-C/W interfaces is confirmed by GIXD measurements. The W_2C content is more important in the case of the W layer deposited at 200 Watts. Moreover, the part of the W layer, which has not reacted with the a-C layer, is crystallized in the α-W phase after the annealing.

Keywords : Carbon; tungsten; interface; tungsten carbide; annealing; X-ray; reflectometry; diffraction; RF sputtering.

I. Introduction

Transition metal carbides, like tungsten carbides, have a considerable technological interest due to their specific physical, chemical and mechanical properties [1]. In thin films technology, they are frequently used as hard and wear-resistant coatings for cutting and drilling tools [1, 2]. Tungsten carbides are also used as electrochemical probes and interconnections in materials designated to be used in severe conditions, such as, sustained temperatures or corrosive environments [2-4]. Reactive sputtering, co-sputtering, laser ablation, and chemical vapor deposition (CVD) are the most techniques commonly used to synthesize tungsten carbides thin films [2, 5]. On the other hand, a-C/W multi-layers are expected to be used in X-ray mirrors technology (see, for example, [6] and references therein). These mirrors are generally fabricated by depositing alternate layers, of high and low atomic number elements, on low roughness substrates. In the present work, we used a technique that consists to deposit a bi-layer structure of carbon on tungsten and then anneal the obtained samples, after deposition, to obtain tungsten carbides. Indeed, annealing of a multilayer structure of two different materials leads to structural properties changes (compaction, period expansion, inter-diffusion and crystallization). Roughness and interdiffusion generally lead to the formation of intermediate layers at the interface and eventually to the formation of compounds [7]. We present, in this work, the structural properties and the interface state of a-C/W bi-layers, deposited by radio frequency (RF) sputtering, before and after annealing at 1000 K for 1 hour.

II. Experimental details

Amorphous carbon on tungsten bi-layers (a-C/W) were deposited, on silicon substrates, by the RF sputtering technique. The deposition system is equipped with an Alcatel oil diffusion pump, which permits a low pressure of 10^{-6} Torr to be regularly achieved before introducing the sputtering gas (pure argon). The argon pressure, during the deposition, is maintained to 10^{-2} Torr. Before their introduction in the sputtering chamber, crystalline silicon substrates have been washed with ethanol, and then, cleaned in an ultrasonic bath of acetone. The a-C films were deposited, from a high purity graphite target, at a power of 250 Watts; while tungsten ones, were obtained from a high purity tungsten target at 100 Watts and 200 Watts. To eliminate eventual surface targets contamination, during air exposition, each target is sputter etched for 15 minutes, prior to the deposition on the silicon substrates. The obtained samples are designated by a-C/W100 and a-C/W200;

where the numbers 100 and 200 represent the RF power used for tungsten films deposition. Annealing, achieved on these samples, has been done under a vacuum pressure of 10^{-6} Torr at 1000 K for 60 minutes. The structural characterization of the samples has been done by Grazing Incidence X-rays Reflectometry (GIXR) and Diffraction (GIXD) techniques using the CuKα radiation.

III. Results and discussion

III-1. X-rays reflectometry

Figure 1 shows the GIXR diagrams obtained on the a-C/W100 and a-C/W200 bi-layers before annealing.

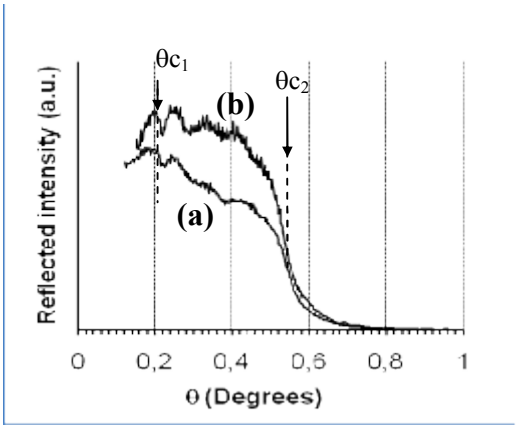

Figure 1 : GIXR diagrams obtained on (a) a-C/W100 and (b) a-C/W200 bi-layers before annealing

The GIXR diagrams present two critical angles, which are located at θ_{c1} = 0,2° and θ_{c2} = 0,54° respectively. The first critical angle θ_{c1}, which corresponds to the penetration of X-rays in the a-C layer, is not well marked because of the small thickness and the low absorption coefficient of this layer. The second one θ_{c2}, which corresponds to the penetration of X-rays in the tungsten layer, is well marked. Below the critical angle of the a-C layer ($\theta_{c1} \approx$ 0,2°), we can note a slight increase of the reflected intensity. This behavior is due to the small size of the samples. Indeed, at very small incidence angles, if the sample size is too small, the incident X-ray beam is not totally intercepted by the surface sample. Then, increasing the incidence angle leads to an increase of the incident beam part intercepted by the sample. Therefore, the reflected intensity increases [8].

For X-ray radiations, the refractive index n is slightly inferior to the unity and the complex refractive index n* of a medium is given by [8-10] :

$$n^* = n - i\beta = 1 - \delta - i\beta \qquad (1)$$

Where β is the extinction coefficient and δ is related to the density, ρ, of the material by the following expression:

$$\delta = (r_0 \lambda^2/2\pi)\, N_A\, \rho(Z+\Delta Z)/M \qquad (2)$$

where r_0 is the classical radius of the electron (r0 = 2.82 10-15 m), λ the wavelength of X-rays, N_A the Avogadro number, Z the atomic number of the element, ΔZ the dispersion correction for atomic scattering factor for the used X-ray radiation [11] and M the atomic mass of the element. The critical angle θ_c is directly related to the density ρ of the analyzed material. It is given, approximately, by the following equation:

$$\theta c = (2\delta)^{1/2} = [(r_0 \lambda^2/2\pi)\, N_A\, \rho(Z+\Delta Z)/M]^{1/2} \qquad (3)$$

Assuming that θ_{c2} is the critical angle of the W layer, with ΔZ = -6 for tungsten [11], the density of this layer, calculated from the relation (3), is 18 g/cm3. This value is very close to those obtained for tungsten single layers deposited in similar conditions. However, it is slightly shifted, towards small values, compared to the bulk tungsten density (about 19 g/cm3). Such behavior is generally observed in thin films and is attributed to the presence of voids and defects [8, 12]. This result indicates that there is no formation of W_xC_{1-x} interfacial layer; otherwise, the critical angle θ_{c2} should be less than 0,54° (and the density less than 18 g/cm^3). This result suggests that the as deposited a-C/W100 and a-C/W200 interfaces are abrupt.

For incidence angles between the critical angles θ_{c1} and θ_{c2}, the GIXR diagrams show interference fringes with three maxima. These fringes are due to interference between waves reflected by the a-C and W layers. A curve fitting of the experimental diagrams, according to the Parrat formalism [13], allowed us to determine the thickness of each layer. The a-C layers thickness is about 40 nm while the W100 and W200 layers thickness is about 85 nm and 75 nm respectively. These thickness values are very close to those expected from the deposition rates of a-C and W films deposited at similar conditions. Therefore, there are no thickness changes, which can be caused by an eventual reactivity at the a-C/W interfaces. This result confirms that the a-C/W100 and a-C/W200 interfaces are abrupt. Otherwise, the a-C layers thickness should be decreased.

Figures 2 and 3 show the GIXR diagrams, obtained on a-C/W100 and a-C/W200 bi-layers, before and after annealing. Compared to the diagrams of the as deposited bi-layers, these diagrams exhibit two significant changes: the interference fringes observed between θ_{c1} and θ_{c2} are almost disappeared and the second critical angle θ_{c2} is shifted towards small angles with a new value θ_{c3} = 0.5°. These results indicate

clearly a considerable decrease of the a-C layers thickness and the formation of a W_xC_{1-x} interfacial layer. This result suggests that, after the annealing, an inter-diffusion of carbon and tungsten occurs at the interface.

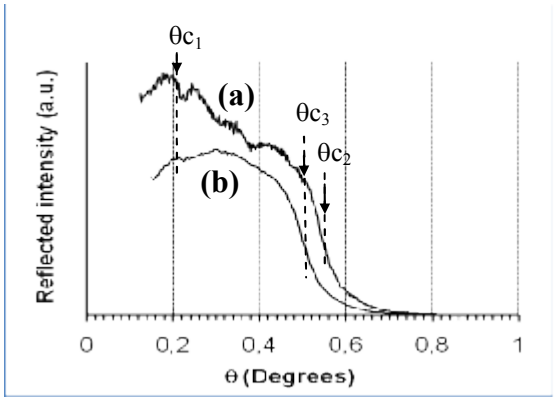

Figure 2 : GIXR diagrams obtained on raw (a) and 1000 K annealed (b) a-C/W100 bi-layer

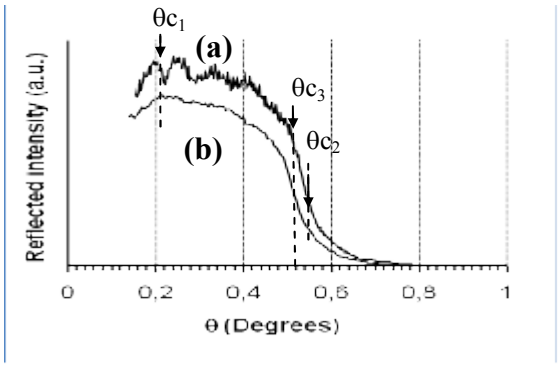

Figure 3 : *GIXR diagrams obtained on the a-C/W200* bi-layer before (a) and after (b) 1000 K annealing

Taking into account that the interfacial compound formed after the annealing is W_2C, as will be revealed by GIXD measurements, the density of the interfacial layer, calculated from the critical angle θ_{C3}, is about 16 g/cm3. Compared to values reported for the bulk W2C density (about 17 g/cm3) [14-18], this value is slightly shifted towards small values, as in the case of the W layers, for the same reasons indicated above. This result suggests that the 1000 K annealing of the a-C/W100 and a-C/W200 bi-layers leads to the formation of a W2C layer at the interface as will be confirmed by GIXD measurements.

III-2. X-rays diffraction

Figure 4 shows the GIXD diagrams obtained on the a-C/W100 and a-C/W200 bi-layers before annealing. The diagram of the a-C/W100 bi-layer presents a broad line, centered at $2\theta = 40°$, which can be attributed to amorphous tungsten. This result suggests that all the a-C/W100 structure is amorphous. The GIXD diagram of the a-C/W200 bi-layer shows three diffraction peaks, located at $2\theta = 35{,}5°$, 40° and 43,8°, which correspond, respectively, to the (200), (210), and (211) lines of the β-W phase [19]. This result indicates that the W200 layer is crystallized in the β-W phase before the annealing.

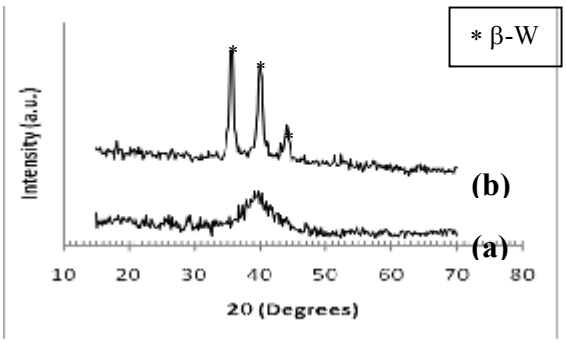

Figure 4 : GIXD diagrams obtained on a-C/W100 (a) and a-C/W200 (b) bi-layers before annealing (for $\theta = 1°$).

Figure 5 shows the GIXD diagrams of the 1000 K annealed a-C/W100 bi-layer for different values of the grazing incidence angle θ. For $\theta = 0.3°$, the GIXD diagram does not show any diffraction peak. This result confirms that the non-reacted part of the carbon layer is still amorphous. Indeed, at this grazing incidence angle, the X-rays beam penetrates only in the carbon layer, and then, it is totally reflected by the W2C interfacial layer. For $\theta = 0.5°$, the GIXD diagram presents mainly two diffraction peaks, located at 34,5° and 39,5°, which can be easily attributed, respectively, to the (100) and (101) lines of W2C [18-20]. This result confirms the formation of W_2C at the a-C/W100 interface, after the 1000 K annealing, as deduced above from the GIXR measurements.

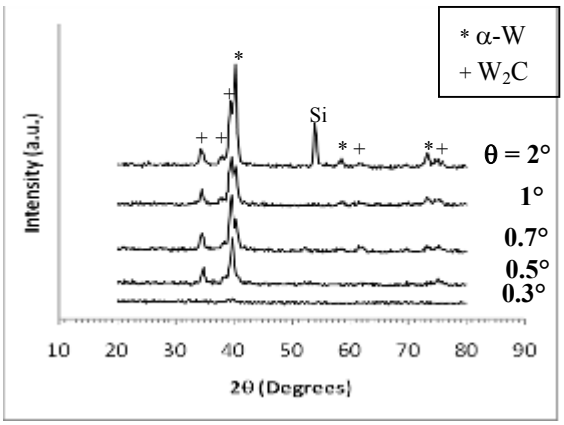

Figure 5 : GIXD diagrams obtained on 1000 K annealed a-C/W100 bi-layer for different grazing incidence angles θ

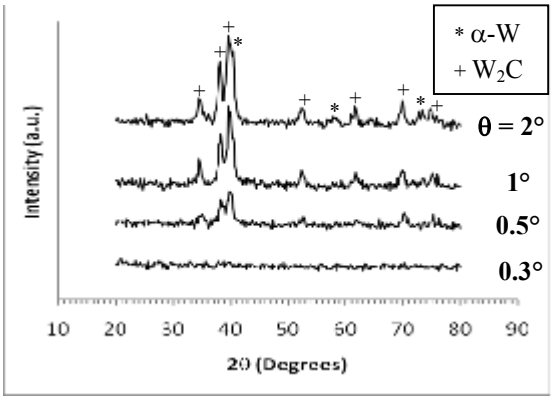

Figure 6 : GIXD diagrams obtained on 1000 K annealed a-C/W200 bi-layer for different grazing incidence angles θ

For greater incidence angles, between 0,7° and 2°, we note the apparition of additional new diffraction peaks, located at 40,5°, 58,3° and 73,3°, which are attributed, respectively, to the (110), (200) and (211) lines of the α-W phase [21, 22]. These peaks become more and more intense as the grazing incidence angle increases. This result indicates that the W100 layer has not entirely reacted with the a-C layer and the non-reacted part is changed from the β-W to the α-W phase.

Furthermore, it should be noted that, after the 1000 K annealing, there is no appearance of any WC diffraction peak. This behavior is probably because the annealing temperature is not sufficient to induce the formation of crystallized WC, which needs relatively higher temperatures [23].

Figure 6 shows GIXD diagrams, of the 1000 K annealed a-C/W200 bi-layer, for different grazing incidence angles θ. As in the case of the a-C/W100 bi-layer, for an incidence angle of 0,3°, the GIXD diagram doesn't show any diffraction peak. For incidence angles greater than θ = 0,5°, the diffraction peaks attributed to W_2C are well observed. On the other hand, as θ increases, the peak at 2θ = 40,5°, due to the α-W phase, begins to appear; but remains always less intense than the nearest W_2C peak located at θ = 39,5°. This result shows that the inter-diffusion is more important than in the a-C/W100 structure case.

IV. Conclusion

Amorphous carbons on tungsten (a-C/W) bi-layers were deposited, on crystalline silicon substrates, by RF sputtering. The obtained samples have been then submitted to a thermal annealing, in vacuum, at 1000 K. Grazing Incidence X-rays Reflectometry (GIXR) and Diffraction (GIXD) techniques were used to study the interface state and the structure of these bi-layers before and after annealing.

The as deposited a-C/W interfaces are abrupt while the annealed ones are diffuse with formation of a W2C interfacial layer. The tungsten films deposited at 100 Watts are amorphous while those deposited at 200 Watts are polycrystalline in the β-W phase. The W_2C content is more important in the case of the W layer deposited at 200 Watts. Moreover, the part of the W layer that has not reacted with the a-C layer is crystallized in the α-W phase after the annealing. At the used annealing temperature (1000K), there is no formation of tungsten carbide, (WC).

V. References

[1] K. Abdelouahdi, C. Sant, C. Legrand-Buscema, J. Perriere, G. Renou and P. Aubert, Surface & Coatings Technology 200 (2006) 6469–6473
[2] B.Q. Yang, X.P. Wang, H.X. Zhang, Z.B. Wang and P.X. Feng, Materials Letters 62 (2008) 1547–1550
[3] P. Dubcek, N. Radic and O. Milat, Nucl. Instr. and Meth. in Phys. Res. B 200 (2003) 329–332
[4] Kh. G. Kirakosyana, Kh. V. Manukyana, S. L. Kharatyana and R. A. Mnatsakanyan, Materials Chemistry and Physics 110 (2008) 454–456
[5] E. Ech-chamikh , M. Azizan , F. Debbagh , A. Essafti and Y. Ijdiyaou, M. J. Cond. Mat, Vol. 9,No.1 (2007)
[6] B.K. Gana, B.A. Latella and R.W. Cheary, Applied Surface Science 239 (2005) 237–245
[7] M. H. Modi, G. S. Lodha, S. R. Naik, A. K. Srivastava and R. V. Nandedkar, Thin Solid Films, 503 (2006) 115-120
[8] A. Biswas, A.K. Poswal, R.B. Tokas and D. Bhattacharyya, Applied Surface Science 254 (2008) 3347–3356
[9] M. Youssef El AZHARI. Thèse d'état, Université Cadi Ayyad-Marrakech (2003)
[10] P. Zaumseil, Materials for information technology, Springer – London (2005) 497
[11] International tables for X-ray crystallography, Kynoch press, England, Vol III, (1962) 201
[12] B.K. Gana, B.A. Latellab and R.W. Cheary, Applied Surface Science 239 (2005) 237-245
[13] L. G. Parratt, Phys. Rev. 95 (1954) 359
[14] J. Luthin and Ch. Linsmeier, Surface Science, (2000) 454-456
[15] J. Zhao, T. Holland, C. Unuvar and Z. A. Munir, Int. Journal of Refractory Metals & Hard Materials 27 (2009) 130-139
[16] M.M. Gauthier, Engineered Materials Handbook, 1995, pp. 961-963

[17] A. Klimpel, A. Lisiecki and D. Janicki, Journal of Materials Processing Technology 164–165 (2005) 1068–1073
[18] D. Bhattacharyya, D. Joseph and A.K. Poswal, Nucl. Instr. and Meth. in Phys. Res. B 248 (2006) 264–272
[19] Michael B. Zellner, Jingguang and G. Chen, Catalysis Today 99 (2005) 299–307
[20] A. Pinyol, E. Bertran, C. Corbella, M.C. Polo and J.L. Andujar, Diamond and Related Materials 11 (2002) 1000–1004
[21] J.C. Sánchez-López, D. Martínez-Martínez, M.D. Abad and A. Fernández, Surface & Coatings Technology 204 (2009) 947–954
[22] S. Bolokang, C. Banganayi and M. Phasha, Int. Journal of Refractory Metals & Hard Materials (2010) 211-216
[23] Y. Hatano, M. Takamori, K. Matsuda, S. Ikeno, K. Fujii and K. Watanabe, Journal of Nuclear Materials 307–311 (2002) 1339–1343